A&A 530, A129 (2011)
DOI: 10.1051/0004-6361/201016033

Astronomy & Astrophysics

On the influence of the Sun on the rapid variability of compact extragalactic sources

N. Marchili[1], T. P. Krichbaum[1], X. Liu[2], H.-G. Song[2], J. M. Anderson[1], A. Witzel[1], and J. A. Zensus[1]

[1] Max-Planck-Institut für Radioastronomie, Auf dem Hügel 69, 53121 Bonn, Germany
e-mail: marchili@mpifr-bonn.mpg.de
[2] Urumqi Observatory, the National Astronomical Observatories, the Chinese Academy of Sciences, Urumqi 830011, PR China

Received 30 October 2010 / Accepted 16 March 2011

ABSTRACT

Since December 2004, we have performed a program to monitor intraday variable sources at a frequency of 5 GHz at the Urumqi Observatory. We present our analysis of the variability characteristics of the flat-spectrum radio source AO 0235+164, which detects an annual cycle in the variability amplitude. This appears to correlate with the solar elongation of the source. A thorough analysis of the results of the MASIV IDV survey – which provides the variability characteristics of a large sample of compact radio sources – confirms that there is a small but detectable component of the observed fractional modulation that increases with decreasing solar elongation. We discuss the hypothesis that the phenomenon is related to interplanetary scintillation.

Key words. scattering – quasars: individual: AO 0235+164 – radio continuum: general – solar wind – surveys

1. Introduction

IntraDay Variability (IDV, see Witzel et al. 1986, Heeschen et al. 1987) refers to the rapid intensity variability – on timescales from a few hours to ~2 days – which affects a considerable number of flat-spectrum radio sources (a fraction between 30% and 50%, see Quirrenbach et al. 1992; Lovell et al. 2008). The variability concerns both total flux density and polarization measurements over a wide range of the electromagnetic spectrum, from the radio to the optical bands.

Both source-intrinsic and source-extrinsic models have been proposed to explain IDV. In the optical bands, the variability should be regarded as intrinsic to the sources (Wagner & Witzel 1995). The origin of the variability in the radio bands has not yet been solved. For the most extreme sources – the so-called fast-scintillators (see Dennett-Thorpe & de Bruyn 2002; Bignall et al. 2003), which have total flux variations of the order of 100% on timescales of hours – the variability is most likely caused by InterStellar Scintillation (ISS), caused by nearby scattering screens located at a distance of several parsecs (see Dennett-Thorpe & de Bruyn 2002; Rickett et al. 2006). However, only a very small fraction of IDV sources can be labelled as fast scintillators. In the Micro-Arcsecond Scintillation-Induced Variability (MASIV) survey (Lovell et al. 2003, 2008), a strong correlation was found between the variability amplitude of a large sample of compact radio sources and the emission measure in the ionized interstellar medium along their respective lines of sight, showing that a significant part of the variability is due to ISS.

The discovery of correlated variations in the optical and radio light curves of S5 0716+714 (Quirrenbach et al. 1991) suggested that at least part of its variability is intrinsic to the source. This then raises the question of how large the contribution of source-intrinsic mechanisms to the total variability is and, even more important, whether the case of S5 0716+714 should be regarded as an exception among IDV sources.

A possible way to investigate the nature of IDV in a given source is to study how its variability characteristics, namely amplitude and timescale, change with time. Following Narayan (1992), we shortly discuss how these quantities vary in the case of IDV caused by ISS. They can both be described in terms of the Fresnel scale, $r_{\rm f}$, and the diffraction scale, $r_{\rm diff}$. The former is given by $r_{\rm f} \sim \sqrt{\lambda D}$, where D is the distance between the observer and the scattering screen. The latter depends on the properties of the screen and the wavelength of the observations; typical values of $r_{\rm f}$ for the interstellar medium are of the order of 10^{10} cm for observations at centimeter wavelengths and screen distances of the order of 10–100 pc. When variability is caused by weak scattering – as one would expect for classical IDV radio sources – and the angular source size $\theta_{\rm s}$ is larger than the Fresnel angle $\theta_{\rm f} = r_{\rm f}/D$, the characteristic variability timescale can be expressed as

$$\tau_{\rm c} \approx \frac{r_{\rm f}}{v}\frac{\theta_{\rm s}}{\theta_{\rm f}}, \tag{1}$$

where v is the relative velocity between the screen and the observer.

For a given time series, a measure of its variability amplitude is given by the modulation index, $m_{\rm i}$, which is the ratio of the standard deviation to the average. For variability caused by ISS, the modulation index of a light curve is given by Narayan (1992) to be

$$m_{\rm i} \approx \left(\frac{r_{\rm f}}{r_{\rm diff}}\right)^{5/6}\left(\frac{\theta_{\rm f}}{\theta_{\rm s}}\right)^{7/6}. \tag{2}$$

The two equations above can be used to predict how the variability characteristics of a source should evolve throughout the year. The timescale of scintillation-induced variability changes with the relative velocity between the scattering screen and the observer. Due to the Earth's motion around the Sun, this velocity follows an annual cycle which should result in an annual

Table 1. Observing sessions of the Urumqi monitoring program in which AO 0235+164 was observed.

Epoch	Day	Duration (d)	N. S.	Duty cycle (data h^{-1})	m_0 (%)	m_i (%)
2006.12.18	718	2.4	12	1.3	0.6	0.62
2007.01.25	755	2.3	14	1.1	0.7	1.67
2007.02.12	773	4.0	15	1.0	0.6	1.53
2007.03.24	813	2.8	16	0.9	0.7	1.95
2007.04.20	840	3.7	16	0.8	0.8	6.28
2007.06.16	897	2.4	16	0.9	0.7	3.01
2007.07.19	930	2.9	18	0.9	0.7	1.78
2007.08.18	960	3.1	15	1.0	0.8	2.44
2007.10.13	1016	3.0	16	0.8	0.5	1.14
2007.12.22	1086	3.2	15	1.0	0.5	2.15
2008.02.25	1151	2.9	15	0.8	0.6	3.00
2008.03.22	1177	3.0	15	1.1	0.5	1.95
2008.04.22	1208	3.1	14	0.9	0.5	6.48
2008.09.12	1351	3.5	14	1.1	0.5	2.16
2008.11.06	1406	3.6	15	0.5	0.7	1.44
2008.12.22	1452	2.4	15	1.0	0.5	0.72
2009.06.26	1638	2.6	16	0.7	0.5	1.11
2009.08.21	1694	4.1	16	0.9	0.5	1.28
2009.09.22	1726	5.5	14	0.9	0.5	1.90
2009.10.09	1743	2.3	15	1.1	0.5	1.02
2009.11.22	1787	3.8	16	0.8	0.6	1.00

modulation of the variability timescale (see Dennett-Thorpe & de Bruyn 2000; Rickett et al. 2001; Gabányi et al. 2007). The modulation index, instead, should not change with time, unless the variability timescale exceeds the total duration of the observations, in which case the detected variability would decrease as the timescale increases.

In 2004, a collaboration between the Max-Planck-Institut für Radioastronomie (MPIfR) and the Urumqi Observatory initiated a project to monitor classical IDV sources (Gabányi et al. 2007; Marchili et al. 2008, 2010). The aim of the project is to study how the variability characteristics of the target sources change with time. Among others, a sample of six well-known IDV sources has been regularly observed with the 25 m-Urumqi radio telescope, at a frequency of 4.80 GHz. These are the flat-spectrum radio sources AO 0235+164, 0716+714, 0917+624, 0954+658, 1128+592, and 1156+295. The project is still ongoing; during February 2010, 42 observing sessions were carried out. The main characteristics of the 21 epochs in which AO 0235+164 was observed are summarized in Table 1: in Col. 1 we report the observing date at half-session, in Col. 2 the corresponding day (0 = January 1st, 2005), in Col. 3 the duration of the observations, in Col. 4 the number of observed sources (including the calibrators), and in Col. 5 the duty cycle (i.e. the average number of data-points per source per hour).

2. Urumqi data

2.1. Observation and data calibration

The observations were performed with the 25-m parabolic antenna of the Nanshan radio telescope, operated by the Urumqi Observatory (for more details, see Sun et al. 2006; Marchili et al. 2010, and references therein). Its single beam dual polarization receiver, built by the MPIfR, is centred at a frequency of 4.80 GHz and has a bandwidth of 600 MHz.

All the flux density measurements were performed in cross-scan mode, each scan consisting of eight sub-scans – four in azimuth, four in elevation – over the source position. This observing mode allows the evaluation and correction of residual small pointing offsets and the detection of non-Gaussian cross-scan profiles in case of in-beam confusion.

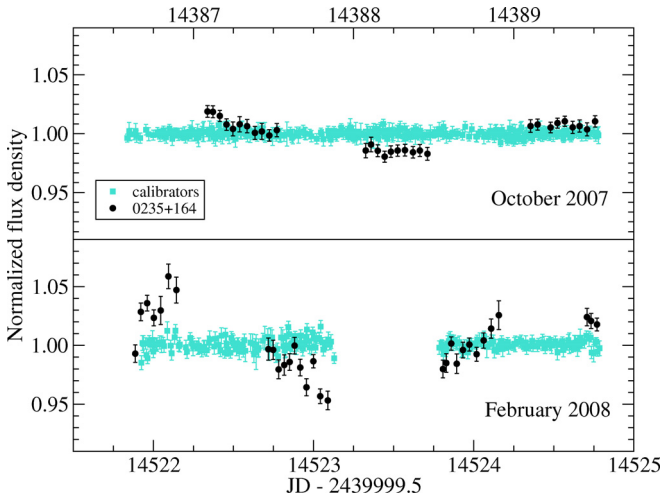

Fig. 1. The variability curves of AO 0235+164 (black dots) in October 2007 (*upper panel*) and February 2008 (*lower panel*), examples, respectively, of a low and a high variability state of the source.

The data calibration procedure follows a standard pipeline. A Gaussian fit to the sub-scans provides an estimate of the flux density. After a quality check, an error-weighted average of the reliable sub-scans provides a flux density measurement for each scan. This value is then corrected for the antenna-gain dependency on both the elevation and the weather conditions, by parameterizing the changes that these effects induce on several calibrators. The accuracy in the flux density measurements can be evaluated using the modulation index of the calibrators, m_0. During normal weather conditions, we find m_0 values of between 0.5% and 0.7%. A more thorough description of the data calibration procedure can be found in Kraus (1997), Marchili (2009), and references therein.

2.2. Variability characteristics of AO 0235+164

The flat-spectrum radio source AO 0235+164 ($z = 0.94$) was found to show variability on IDV timescales more than once in the past (see, e.g., Kraus et al. 1999); Senkbeil et al. (2008) reported a likely extreme-scattering-event in AO 0235+164 in July 2005. The source was observed with the Urumqi radio telescope in 21 epochs between December 2006 and November 2009. Two of the collected light curves are shown in Fig. 1. In Table 1, for each observing session we summarize the calibration accuracy (m_0; Col. 6) and the variability amplitude of AO 0235+164 (Col. 7) in terms of the modulation index m_i. The uncertainties in m_i – evaluated by means of synthetic light curves with the same sampling as the original curves – range between 10% and 20% of the m_i estimations.

2.3. Annual variation in the modulation index of AO 0235+164

Plotting m_i versus the date of the observation, it appears that the modulation index of AO 0235+164 (black dots in Fig. 2, lower panel) follows a regular pattern. The variability seems to be more intense between February and August than between September and January. To investigate this effect, we applied a Lomb-Scargle periodogram analysis (see Lomb 1976; Scargle 1982) to m_i, which identified a periodic oscillation with a period of one year (see Fig. 3).

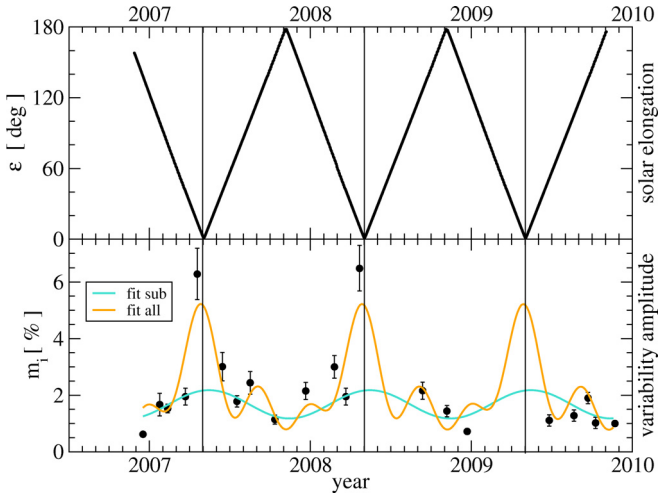

Fig. 2. Solar elongation (*upper panel*) and modulation index (*lower panel*) of AO 0235+164 plotted versus observing time. The orange line shows the sum of the three variability components which correspond to the harmonics of the signal highlighted in the periodogram analysis in Fig. 3. The cyan line shows a sinusoidal fit obtained after removing the data-points corresponding to the two epochs at smallest solar elongation.

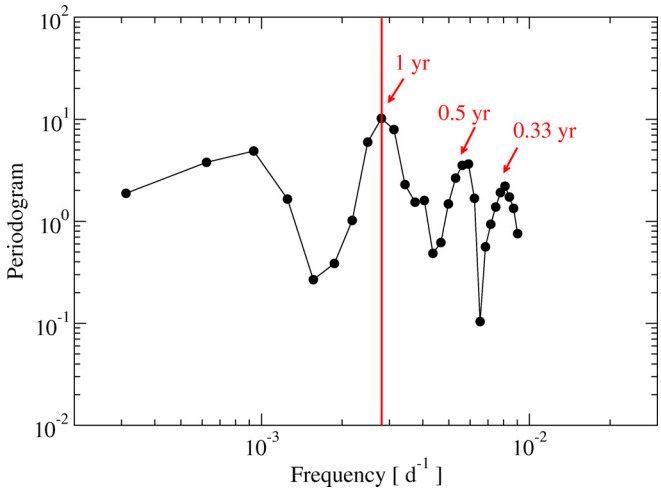

Fig. 3. Periodogram analysis of the variability amplitudes m_i of AO 0235+164. Four peaks of power are clearly visible; three of them correspond to periods of 1, 1/2, and 1/3 of year (red arrows), i.e., the first three harmonics of a one-year periodic signal. This is strong evidence in favour of an annual cycle in the variability amplitude of the source.

We summed the variability components corresponding to the three harmonics of the signal, which are indicated in the periodogram analysis in Fig. 3. This step allows us to estimate the amplitude and phase of the periodic oscillation. The annual cycle (orange line in Fig. 2, lower panel) peaks at the time of the year in which the solar elongation of AO 0235+164, ϵ_{0235}, is at the minimum (see Fig. 2, upper panel). The yearly variation observed in m_i has a large amplitude in both 2007 and 2008. In 2009, the modulation is clearly not visible possibly because of the lack of observations between January and July, which is the time span across which we would expect the largest variations. However, we note that between 2008 and 2009 the solar activity was very low, because of the transition from the 23rd to the 24th solar cycle. In this sense, the absence of significant changes in the variability amplitude of AO 0235+164 may support the hypothesis that these changes are related to the solar activity, hence induced by the Sun.

Two measurements of m_i stand out from the others, which correspond to the observing sessions performed in April 2007 and April 2008. During those epochs, the solar elongation ϵ_{0235} was relatively small (~13° and ~11°, respectively). We repeated the periodogram analysis excluding the two data-points with $\epsilon_{0235} < 30°$, to establish whether the increase in the m_i value is limited only to the epochs of small solar elongation. We found that a periodic oscillation with a period of about one year is still clearly detectable. A sinusoidal fit to these data (see Fig. 2, lower panel, cyan line) shows that the oscillation has a peak-to-peak amplitude of ~1.1%, while the average m_i value is ~1.7%. The increase in m_i between the time of maximum and minimum solar elongation is of the order of 90%. This implies that, during our observations, the solar elongation plays the main role in the variability of AO 0235+164. The phase of the periodic signal is slightly offset (~10 days) with respect to the time of the year of minimum elongation. This offset, however, is much smaller than the average time separation between consecutive observing sessions (~50 days). We can conclude that periodic variations correlated to solar elongation affect the modulation index of AO 0235+164 even for solar elongation ϵ_{0235} larger than 30°.

2.4. Variability timescale

At first glance, an annual cycle in the modulation index of an IDV source may appear to be related to an annual modulation in its variability timescales. As explained above, m_i could undergo yearly-periodic changes if the variability timescale exceeds the duration of the observations. In this case, the variations in τ_c and m_i should be anti-correlated. We can check this hypothesis by studying how τ_c changes as a function of m_i. For each observing session, we estimated the characteristic variability timescale of AO 0235+164 by applying to the light curves three different kinds of time analysis methods, namely a first-order structure function analysis (see Simonetti et al. 1985), a wavelet-based algorithm (Marchili et al., in prep.), and a sinusoidal fitting procedure. The uncertainties in the timescales are mostly due to the limited duration of the observations, obs_d. We estimated that these are proportional to $(\tau_c{}^{3/2})/(obs_d)^{1/2}$. The proportionality factor has been calculated by looking at the distribution of the peak-to-peak timescale – the time interval between a local minimum (or maximum) and the following maximum (or minimum) – for a few light curves characterized by fast variability.

In Fig. 4, we plot the variability timescales versus m_i for all the epochs in which the source showed significant variability (i.e. the probability of a constant flux density was lower than 0.1%, according to a chi-square test). A cycle in m_i as strong as the one we observed in AO 0235+164 should result in a clear increase in τ_c as m_i decreases. The plot, however, does not reveal such a trend. In particular, while the extreme variability observed in April 2007 is characterized by a value of τ_c among the highest detected in the source, the one for the April 2008 observations is quite low (see Fig. 5). This leads to the conclusion that the annual cycle in m_i cannot be explained in terms of an annual modulation of the variability timescale.

3. MASIV data

Given the large number of sources it comprises, the MASIV survey seems to be the ideal test ground to investigate the possible correlation between the variability characteristics of compact radio sources and their solar elongation.

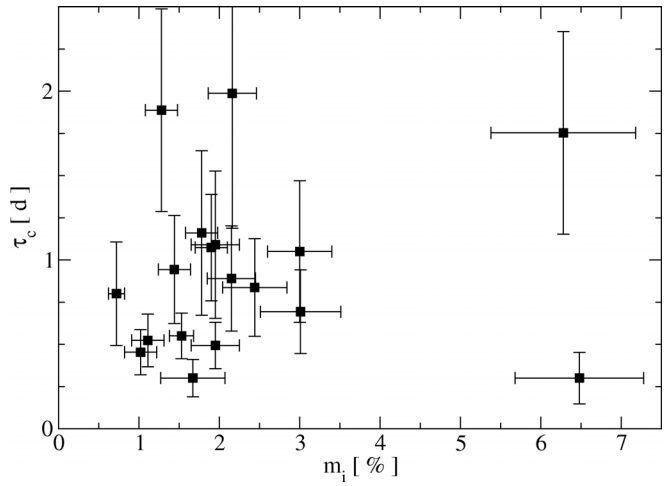

Fig. 4. The variability timescales of AO 0235+164 plotted versus m_i.

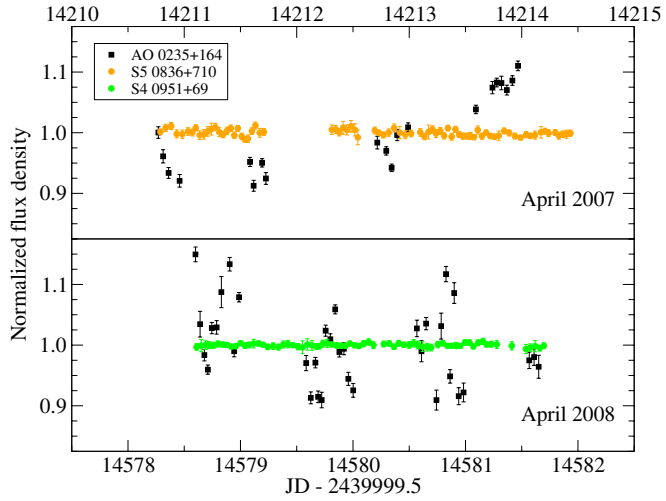

Fig. 5. The variability curves of AO 0235+164 (black squares) in April 2007 (*upper panel*) and April 2008 (*lower panel*), compared with the curves of the calibrators S5 0836+710 (orange dots) and S4 0951+69 (green dots). The timescale of the variability in the two epochs differs considerably.

MASIV is a survey of 710 radio sources, undertaken at a frequency of 4.9 GHz at the Very Large Array (VLA) between January 2002 and January 2003. The main aim of the project was to provide a large sample of scintillating sources for reliable statistical investigation. A core sample of 578 sources was observed in four epochs of three or four day durations, starting on January 19, May 9, and September 13 in 2002 and January 10 in 2003. The results of these observations, along with a detailed description of the observing strategy and data calibration, are reported in Lovell et al. (2008). After removal of the sources that have structure on VLA arcsecond scales or are partially resolved, 475 point sources remained. Basic information about the sources, their flux density, and the raw modulation index for each of the four epochs are provided by Lovell et al. (2008), and are available in the electronic edition of the *Astrophysical Journal*.

We used the modulation indices resulting from the MASIV survey to check whether the data support the hypothesis of an additional contribution to the variability, related to solar elongation. We also checked whether this effect depends on the ecliptic latitude of the sources, as it would be reasonable to expect.

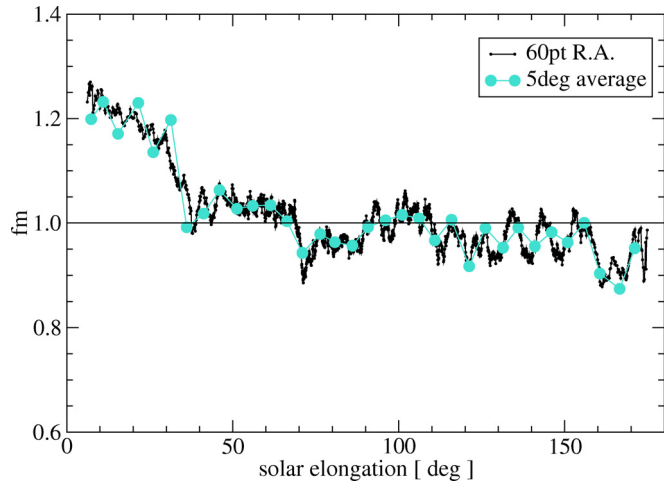

Fig. 6. Results of a 60-point running average on the combined fractional modulation index of MASIV sources (black line) plotted versus solar elongation. The cyan dots show a 5-degree average. The increase in the variability amplitude for $\epsilon < 30°$ is remarkable.

3.1. Modulation index variations as a function of solar elongation

We labeled the four epochs of MASIV observation chronologically, as t_j $\{j = 1, ..., 4\}$. For each session and source, we calculated the solar elongation $\epsilon_{\mathrm{src},j}$. We also defined a new parameter, the fractional modulation index, as

$$fm_{\mathrm{src},\,j} = \frac{m_{\mathrm{src},\,j}}{\langle m_{\mathrm{src}} \rangle} \tag{3}$$

where $m_{\mathrm{src},\,j}$ is the modulation index at the epoch t_j and $\langle m_{\mathrm{src}} \rangle$ is the average modulation index over the four observing sessions. Using the fractional modulation index, we can compare the changes in the variability amplitude of sources with very different variability characteristics. Adopting a statistical approach, the fm values were combined, to study how the variability amplitude changes, on average, as a function of ϵ. We excluded from the analysis the light curves used to calibrate the data (Bignall, priv. comm.), because their modulation index is artificially low.

If the effect observed in AO 0235+164, described above, is common to compact extragalactic sources, we expect to see an increase in fm as ϵ approaches zero. At first sight, the scattering in the individual fm values is too high to reveal a clear trend. A 60-point running average over the data (see Fig. 6, black line) demonstrates the existence of such an increase. In cyan dots, we also plotted the 5-degree average, which confirms the behaviour of the running average. The averaged fm peaks at $\epsilon \sim 10°$ with a value of ~1.25, while the minimum falls close to $\epsilon \sim 165°$ with a value of ~0.9. Most remarkably, all the averaged fm values for $\epsilon < 35°$ are $\gtrsim$1.15, while for $\epsilon > 110°$ most of the values are <1.0. We conclude that solar elongation exerts a considerable influence on the variability of compact radio sources.

In the MASIV survey, the contribution of the solar-elongation related effect to the total variability should not have very serious implications for its main findings. In particular, all the results obtained by using the structure function at a time lag of two days (D(2 days) in Lovell et al. 2008) as an estimate of the source variability should be only marginally affected. This is because D(2 days) is calculated over all the four observing sessions. On the basis of Fig. 6, given a 30−40% enhancement in the modulation index between maximum and minimum solar

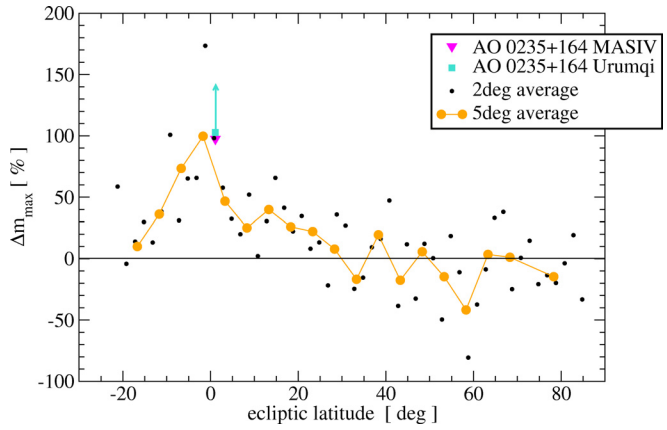

Fig. 7. The modulation index change, Δm_i, as a source passes from the farthest to the closest point to the Sun plotted versus ecliptic latitude β. The two-degree (black dots) and five-degree average (orange dots) pinpoint the large increase in variability for sources with low β. The variation deduced from Urumqi observation for AO 0235+164, plotted as a cyan square, has been obtained excluding the April 2007 and April 2008 observations, and should be regarded as a lower limit.

Table 2. Mean fractional modulation index of the four MASIV observing sessions.

Epoch	$\bar{fm}$	$\bar{fm}(\lvert\beta\rvert < 15°)$	$\bar{fm}(\lvert\beta\rvert > 45°)$
January 2002	0.92	0.85	1.04
May 2002	1.10	1.18	1.03
September 2002	1.11	1.17	1.05
January 2003	0.87	0.80	0.88

Notes. The average fractional modulation index is compared with the averages for the subsamples of source with $|\beta| < 15°$ and $|\beta| > 45°$.

elongation, the additional contribution from the solar elongation effect to the four-epoch combined variability would be of the order of 10% of the total fractional variation for sources observed at low solar elongations.

3.2. Dependence on ecliptic latitude

Any influence of the solar elongation should be particularly prominent for sources at low ecliptic latitude, because of the large solar elongation range that they cover. We define ϵ_{min} and ϵ_{max} as the minimum and maximum solar elongation for a given source during the year. We expect $m_i(\epsilon_{min}) - m_i(\epsilon_{max})$ (from now on, Δm_{max}) to increase as the ecliptic latitude β tends to zero, and to verify this hypothesis, for each source in the MASIV catalogue we applied a linear regression to the four m_i values as a function of ϵ. The regression coefficient A was used to estimate the variation in the modulation index by evaluating

$$\Delta m_{max} = A\ (\epsilon_{min} - \epsilon_{max})\,. \quad (4)$$

The Δm_{max} values obtained for all sources, averaged in bins of two (black dots) and five (orange dots) degrees, are presented in Fig. 7, where Δm_{max} is clearly β-dependent. For sources at $\beta \sim 0°$, Δm_{max} is of the order of 100%, decreasing on both sides of the β axis until reaching a value close to 0% at $\beta \sim 30°$.

The calculation of the mean fractional modulation index values at different epochs reveals an interesting characteristic. The averages for the January 2002 and 2003 epochs are systematically smaller than in May and September of 2002. The measured values are shown in Table 2 (Col. 2). This result needs to be carefully examined. The distribution of the sources as a function of solar elongation changes during the year. In January, the Sun is at low declination. Since the MASIV survey includes only sources above declination 0°, in January the average solar elongation is considerably higher than in both May and September. As a consequence, a systematic bias in the measured modulation indices at different epochs – whatever the cause – could in principle emulate a solar elongation dependence of the variability. Conversely, a solar elongation dependence of the variability would affect the average modulation indices measured at different times of the year. If the first hypothesis is correct, the average values of fm should not depend on β. If the second hypothesis is correct, the differences in fm at different epochs should be very pronounced for sources at low β, and negligible for those at high β.

The fm averages for two subsamples of sources at low (<15°) and high (>45°) ecliptic latitude are reported in Table 2, Cols. 3 and 4, respectively.

It appears that the fractional modulation index is strongly β-dependent even within a single observing session, which confirms the existence of a solar-elongation related effect. The similarity between the averages at high β for January, May, and September 2002 seem to indicate that the low average fm value in January 2002 is mainly due to solar elongation. In the case of January 2003, instead, the low fm values at both low and high β cannot be solely ascribed to a solar elongation effect.

We compared the fm averages in Col. 2 of Table 2 with the number of variable sources, N_{var}, detected in each epoch, reported in Fig. 5 of Lovell et al. (2008). The value of N_{var} increases by ~20% from January 2002 to May, by a few percent from May to September and decreases by ~25–30% from September to January 2003. This is in excellent agreement with the behaviour of the fm averages, confirming that the solar-elongation-related effect contributes significantly to the variability observed in MASIV sources.

3.3. Comparison of MASIV and Urumqi results

We compared the results obtained from the MASIV sample with the ones from the Urumqi observations. AO 0235+164 has an ecliptic latitude $\beta \sim 1°$ and was observed in both the MASIV survey and the Urumqi IDV monitoring project. In the first case, we find a Δm_{max} value of 97% (plotted in Fig. 7 as a purple triangle), in excellent agreement with the source-averaged Δm_{max} at $\beta \sim 0°$, which is 98%. If we calculate in a similar way the Δm_{max} for the Urumqi observations (cyan square in Fig. 7), we find values ranging from ~90 to almost 400%, depending on whether the April 2007 and 2008 epochs are excluded from the calculation or not. The exceptional increase in the variability observed in Urumqi for $\epsilon \sim 10°$ cannot be confirmed by the observations of AO 0235+164 in the May epoch of MASIV, when the solar elongation of the source was below 10°.

4. Discussion

Our combined analysis of Urumqi and MASIV results has provided sufficient confirmation of a source of variability related to solar elongation. The nature of the variability, however, remains unclear. We propose some possible explanations below. The discussion of the different models is based on the results of the Urumqi observations, for which we have been able to estimate both the amplitude and the timescales of the variability.

4.1. Weak scattering

Assuming that the variability is caused by weak scattering, we can use Eqs. (1) and (2) to determine the conditions required to reproduce the variability characteristics we observed – namely, $m_i \sim 1-10\%$ and $\tau_c \sim 10^4-10^5$ s. Assuming a scattering screen at 1 a.u. distance, we can calculate a Fresnel scale $r_f \sim 10^2$ km and a Fresnel angle $\theta_f \sim 10^2$ mas. The only parameters we can modify to obtain the proper timescale are the angular size of the emitting region θ_s and the relative velocity between the screen and the observer, v.

Setting a velocity of the order of the solar wind speed ($\sim 10^2$ km s^{-1}) would lead to $\theta_s \geq 10^4\,\theta_f$, which means 100″ at least. Looking at the full-width at half maximum of cross-scans obtained with the Urumqi and Effelsberg radio telescopes, we can rule out this hypothesis.

Assuming θ_s to be of the order of milliarcseconds or smaller (see, e.g., Lazio et al. 2008; Qian & Zhang 2001), the source must be regarded as point-like, and the factor θ_s/θ_f in Eqs. (1) and (2) can be substituted with one. The available constraint on the variability timescale implies that $v \leq 10^{-2}$ km s^{-1}. This is three orders of magnitude lower than the Earth's orbital velocity, which, reasonably, should provide a lower limit to v.

It is well-known that InterPlanetary Scintillation (IPS) contributes to the variability of compact radio sources (Readhead 1971). IPS causes variations in the scintillation index (the standard deviation in the flux density over an ensemble of measurements, which is equivalent to m_i) that depend on solar elongation. This effect is most prominent at low observing frequencies. Following Readhead (1971), for ϵ between ~3° and ~90°, frequencies between 81.5 MHz and 2.7 GHz, and the regime of weak scattering, the dependence of m_i on $\sin\epsilon$ and the frequency ν can be described as a power law

$$m_i(\nu)\,\nu \propto (\sin\,\epsilon)^{-1.55}. \quad (5)$$

Extrapolating this result to a frequency of 4.8 GHz, and using a proportionality factor of 0.22 (see Readhead 1971) gives, for sources with $\epsilon < 30°$, a value of m_i of the order of 1−10%, which is consistent with our results. The timescale of IPS variations, however, is of the order of seconds, at least 10^4 times smaller than the ones that characterize the Urumqi light curves.

4.2. Strong scattering: refractive scintillation

We hypothesize that the variability is due to refractive scintillation. For extended sources, the timescale and modulation index of the variability are given by

$$\tau_{ref} \approx \frac{r_{ref}}{v}\frac{\theta_s}{\theta_{scatt}} \quad (6)$$

and

$$m_{i,ref} \approx \left(\frac{r_{diff}}{r_f}\right)^{1/3}\left(\frac{\theta_{scatt}}{\theta_s}\right)^{7/6}, \quad (7)$$

where $r_{ref} = {r_f}^2/r_{diff}$ and $\theta_{scatt} = r_{ref}/D$. The factor θ_s/θ_{scatt} can be replaced with one when $\theta_s < \theta_{scatt}$. For $\theta_{scatt} > \theta_f$, we can assume this condition to be true when dealing with interplanetary scintillation of compact radio sources. Using Eqs. (6) and (7), we calculated the values of v and r_{diff} that are consistent with the observed variability characteristics (a modulation index of a few percent and $\tau_c \sim 10^4-10^5$ s), which are plotted in Fig. 8. The range of values that are consistent with the solar wind speed

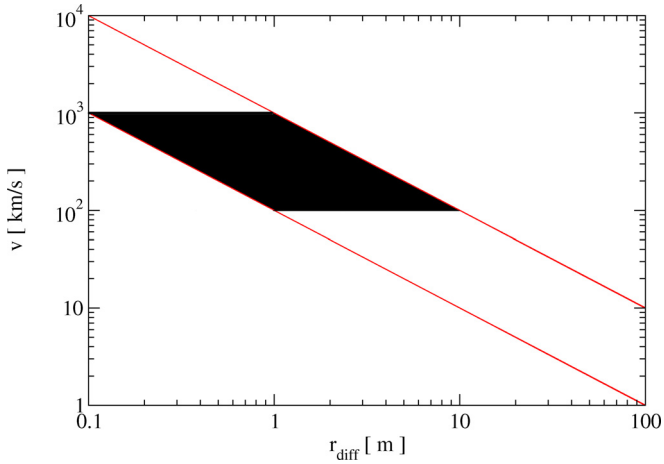

Fig. 8. Between the red lines, the range of values r_{diff} (x-axis) and v (y-axis) are consistent with the variability characteristics observed in the Urumqi data. In black, we indicate the subset of values in the v-range 10^2-10^3 km s^{-1}, corresponding to the solar wind speed.

are marked in black. It appears that to explain the detected variability in terms of refractive scintillation we must hypothesize the existence of density inhomogeneities in the solar wind on a spatial scale of tens of meters or less. Previous studies (see, e.g., Narayan et al. 1989; Coles et al. 1991) refer to an inner scale of turbulence of the order of kilometers.

4.3. Scattering in the Earth's bow shock

The sharp increase in the fractional modulation index at solar elongation close to 30° is compatible with another hypothesis, namely that the variability increases because of propagation effects in the region where the solar wind and the Earth's magnetosphere meet, i.e., the Earth's bow shock. Here the solar wind speed drops considerably because of the interaction with the Earth's magnetic field. It is worthwhile to investigate which values of v and r_{diff} would be required to explain the variability characteristics we found, by assuming a screen at a distance of $\sim 10^8$ m, which is consistent with the approximative distance to the bow shock. This results in a Fresnel scale of $\sim 10^3$ m and a Fresnel angle of the order of arcseconds, which implies that all the sources can be treated as being point-like. For weak scattering, a variability timescale of $\sim 10^4$ s leads to a velocity v of the order of a few m/s – very low, even for the bow shock – while from a modulation index of the order of 1% we can infer that $r_{diff} \sim 10^5$ m. In contrast, for refractive scintillation, the constraints on m_i and τ_c would lead to $r_{diff} \simeq$ m and, consequently, $v \sim 10^2$ km s^{-1}. The value of r_{diff}, in this case, is much smaller than we would expect.

4.4. Correlation between short- and long-term variability

As shown above, both the hypotheses of weak and strong (refractive) scattering can hold only by assuming either a very slow-moving component of the solar wind or irregularities in the interplanetary plasma on very small size scales. For typical parameters of the interplanetary plasma, instead, IPS should cause variability on timescales of seconds. Since the Urumqi observations are performed through sub-scans of a duration of about 30 s, an IPS effect would likely appear as an additional component of noise superimposed on the Gaussian profile of the flux density measurements. An increase in the noise caused by IPS

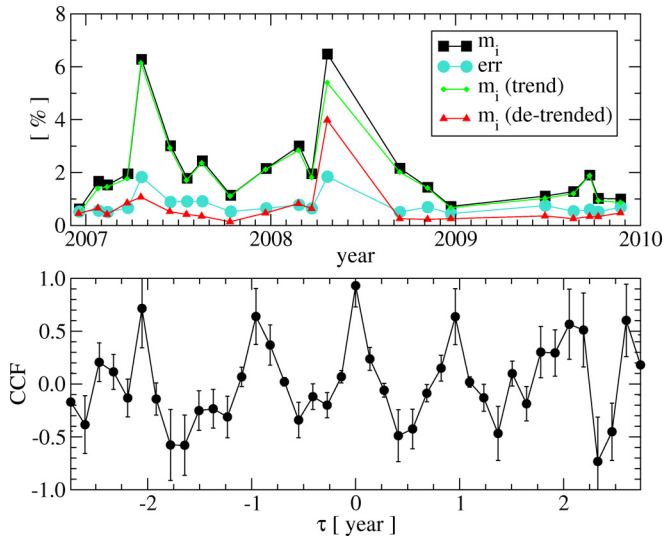

Fig. 9. *Upper panel*: the modulation index (black dots) and the average flux density measurement errors (cyan dots) of AO 0235+164 plotted versus time. The errors are given in percentage with respect to the average flux density of the source during the about three years of observation. The green squares and red triangles show the modulation index of the slow and fast variability component, respectively. *Lower panel*: the correlation function between the modulation index and the flux density measurement errors.

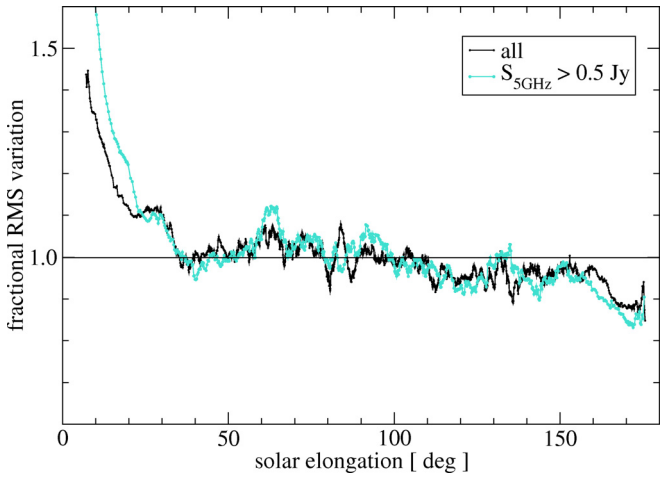

Fig. 10. The 50-point running averages of the fractional rms of the error-in-the-mean for all the MASIV sources (black line) and for a subsample of strong sources (cyan line). The solar elongation dependence is more pronounced in the latter ones.

should translate into a larger uncertainty in the flux density measurement.

For all the observing sessions, we estimated the mean error in the flux density measurements derived from the single sub-scans. We attempted to verify whether the variations in the modulation index could be associated with similar variations in the flux density measurement error. We note that in the error estimation there is a component that depends on the flux density. This component can vary considerably for a strongly variable source such as AO 0235+164 and must be removed. We used the calibrators to derive the proportionality factor, $\alpha_{\rm n}$, between the flux density (S) and the error (ΔS). The flux-independent error for AO 0235+164 was estimated to be $(\Delta S)' = \Delta S - \alpha_{\rm n} S$. The results are presented in the upper panel of Fig. 9. The cyan dots show the ratio of the errors to the average flux density of AO 0235+164 calculated over approximately the past three years of observations, expressed as a percentage. This is meant to provide an estimate of the contribution of flux-independent error to the measurement uncertainty. This contribution is small compared to the variability on longer timescales, estimated from the modulation index (black dots in Fig. 9). However, a locally normalized discrete correlation function (see Edelson & Krolik 1988; Lehar et al. 1992) between the two parameters shows a very high degree of correlation (Fig. 9, lower panel), higher than 0.9. It is also remarkable to discern the peaks of correlation for time lags of ±1 and ±2 years, which confirm the one-year periodical nature of the variations in both the parameters.

We hypothesize that the measurement error directly affects the modulation index by introducing uncorrelated noise in the flux density estimation, which is in turn caused by the uncertainty in the measurements. The periodic increase in the modulation index would correspond to an equivalent increase in the contribution of uncorrelated noise to the overall variability. This, however, is not the case. Since uncorrelated noise has a timescale that must be of the order of the average sampling of the light curves, it can be isolated by separating the very fast variability from the slow one throughout a de-trending procedure (see Villata et al. 2002). The variability amplitude of the de-trended data (red triangles in Fig. 9, upper panel) provides us with an upper limit to the contribution due to the measurement uncertainty. The comparison between the modulation index of the de-trended light curves and those of the long-term trends (green squares in Fig. 9, upper panel) demonstrates that the measurement uncertainty plays a marginal role in the total variability, except maybe for the December 2006 and April 2008 observing sessions. Once we excluded that the measurement error directly affects the modulation index, we can conclude that the short- and long-term variability correlate because they are caused by the same process.

In the MASIV data, any variability on IPS timescales may be investigated by looking at the rms error-in-the-mean for each scan. This is calculated from the scatter in the visibilities over all sub-integration times (typically 18 per one-minute scan, Bignall, priv. comm.) and all baselines (typically ten). The rms errors-in-the-mean for all the scans were kindly provided by Lovell. Following the same approach as in Eq. (3), we calculated for each source the fractional rms error-in-the-mean of each observing session, and plotted it as a function of solar elongation. Its 50-point running average is shown in Fig. 10 (black line). The parameter follows a similarly increasing trend as the modulation index, showing a prominent increase in the fractional variation for solar elongations ϵ below 35°. The solar elongation dependence of the rms is remarkably more pronounced in the stronger MASIV sources ($S_{5\ \rm GHz} > 0.5$ Jy, cyan line in the figure). While for low flux-density sources the rms scatter on very short timescales is mainly due to thermal noise and confusion, for strong sources it is dominated by IPS.

For each MASIV light curve, we separated the long-term trend (which carries information about the variability on timescales of one day or more) from the fast variability component, calculating the modulation index of both. We repeated the analysis presented in Fig. 6 for the trend and the de-trended data separately. The results, plotted in Fig. 11, show a strong solar-elongation dependence in the short-term variability (green line). A similar trend, weaker but still important, also appears in the long-term variability (black line), as a 15-degree average (cyan squares) clearly shows. This suggests that the influence of the

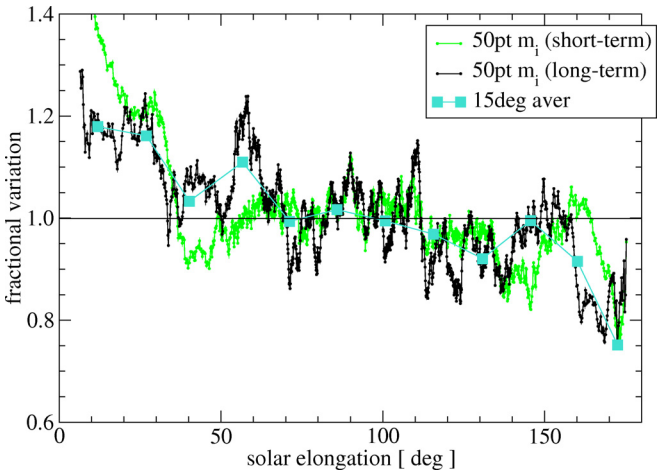

Fig. 11. 50-point running averages of the fractional modulation index of both the long- (black line) and the short-term variability (green line) in the MASIV data. The cyan squares show a 15-degree average on the long-term data.

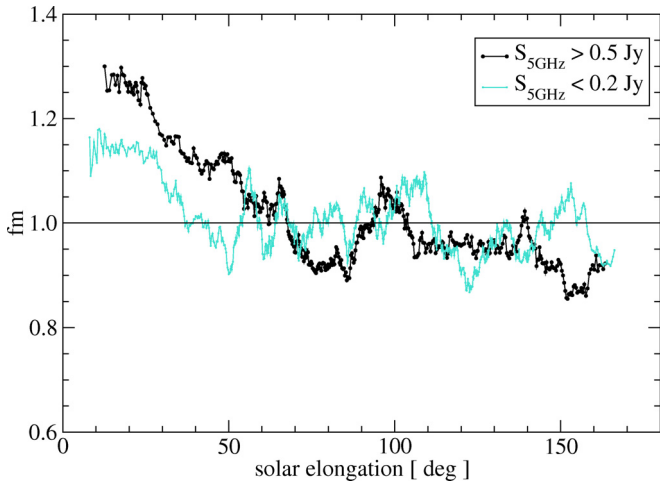

Fig. 12. Results of a 40-point running average on two subsets of MASIV sources. The black curve concerns sources with $S_{5\ \mathrm{GHz}} > 0.5$ Jy, the cyan line sources with $S_{5\ \mathrm{GHz}} < 0.2$ Jy. For strong sources, the solar-elongation dependence of the variability is much more prominent than for weak sources.

Sun on the variability of compact sources goes far beyond the typical IPS timescales.

The hypothesis that the variability of AO 0235+164 is related to IPS is strengthened by the results discussed above. They can be summarized as follows: solar-elongation-related variability on IPS timescales appears in both the Urumqi and the VLA data. Looking at the Urumqi observations, we found evidence that this fast variability component correlates with the variability on typical IDV timescales. To explain the phenomenon in terms of IPS, we would need to postulate the existence of an *atypical*, long-term manifestation of IPS. A possible explanation would be that the variability on timescales of seconds do not introduce a random error in the flux density measurement. We could hypothesize that the scattering causes the flux density of the source to be underestimated, by increasing the opacity of the scattering medium. In this case, a stronger scattering due to a more turbulent medium close to the Sun would lead to lower values of the measured flux density. Changes in the average conditions of the medium along the line-of-sight, which could reasonably take place on timescales of hours or more, or changes in the line-of-sight itself, would appear as a long-term trend in the light curve of the source. A possible confirmation of this picture may come from the results of a study about extreme scattering events, reported by Lazio et al. (2001). Using the Green Bank Interferometer, the authors monitored 149 compact radio sources with an average sampling of about one data-point every two days. They found evidence of a remarkable decrease (10−20%) in the 2 GHz flux density of 0952+179 in two separate occasions. Both events happened when the source was at low solar elongation. The timescales of the variations were of the order of weeks, which would be compatible with the long-term manifestation of IPS hypothesized above. At a frequency of 8 GHz, however, the drop in flux density was not seen.

The existence of a correlation between slow and fast variability may also open the way to a completely different explanation. Observations performed close to the line-of-sight of the Sun may be strongly affected by atmospheric effects (e.g., turbulence in the ionosphere). These are usually ignored because of their short timescales, but if a connection between short and long timescale variability were found in the interplanetary medium, the same could also be true for the atmosphere.

In Sect. 3.3, we underlined that the Δm_{max} value obtained for AO 0235+164 from all the Urumqi observations (i.e. including the two April sessions) is much higher than the one obtained from the MASIV data. This could be caused by changes occurring in either the source structure or the scattering screen during the few years that separate the experiments; but it could also be caused by the difference between the facilities, in the sense that the Urumqi telescope may be more sensitive to the effect than the VLA. This may indicate that there is a possible technical problem. An obvious candidate would be the effect of solar radiation on either the sidelobes of the telescope or the receiver, although this hypothesis appears to be invalid. If we repeat the analysis shown in Fig. 6 on sub-samples of strong and weak MASIV sources (with $S_{5\ \mathrm{GHz}} > 0.5$ Jy and <0.2 Jy, respectively; see Fig. 12), we find that the former are considerably more affected than the latter ones. This is consistent with the results concerning the rms error-in-the-mean of the scans, discussed above. An additional contribution to the variability of the solar radiation should have appeared more clearly in the light curves of weak sources. Furthermore, the solar radiation would be expected to introduce flux density fluctuations that are comparable for sources of similar brightness. In contrast, the large variations observed in the modulation index of AO 0235+164 do not appear in CTA 21, a steep-spectrum source only a few degrees away from AO 0235+164 and similarly bright. At a solar elongation of ∼20°, the modulation index of CTA 21 is of the order of 0.5%.

Another possible technical problem that could affect flux density measurements and depend on solar elongation is the pointing error. Reporting the discovery of flickering in compact radio sources, Heeschen (1984) specified that a considerable number of flux density measurements were excluded from the analysis because of the increase in the pointing errors at low solar elongations. We calculated the average pointing offsets for all the AO 0235+164 Urumqi observations. The April 2007 pointing offset turned out to be the second lowest in the time span between 2005 and May 2007, when the pointing model of the telescope was changed. In April 2008, the pointing offset was lower than the average one calculated between 2007 and 2010. This suggests that a pointing problem cannot account for the solar-elongation-related variability observed in Urumqi.

4.5. The AO 0235+164 variability characteristics in April 2007 and 2008

We highlight again the large difference between the characteristic timescales of AO 0235+164 in April 2007 and April 2008. While in the first epoch most of the variability is due to a slow component ($\tau_c \sim 2$ days), the April 2008 light curve is characterized by a variability timescale comparable to the average sampling (τ_c of the order of one hour, see Fig. 5). As already mentioned, this may indicate that the variability characteristics of the latter are dominated by the uncertainty in the flux measurements. The large amplitude variations observed in AO 0235+164 during the two epochs may be caused by effects that are correlated, but not the same. Further observations are needed to help ascertain the solar elongation at which the fast variability component starts to dominate over the slow one, if and how these variability components can be influenced by either the activity of the Sun or the characteristics of the observing facility.

It cannot be excluded that the conditions in the source itself have to be taken into consideration. In contrast to April 2008, AO 0235+164 in April 2007 was in a flaring state (see Raiteri et al. 2008). The ejection of a strong and very compact emitting component could have caused an additional variability contribution with a characteristic timescale of two days that is caused by ISS. The superposition of the variability contributions due to IPS and ISS could be the origin of the difference between the variability timescales in the two epochs.

5. Summary

We have reported the discovery of a seasonal cycle in the amplitude of the variability in the IDV source AO 0235+164 during the approximately three years of monitoring performed at the Urumqi Observatory. The variability peaks at the time of minimum solar elongation of the source, suggesting that interplanetary scintillation is a possible cause of the phenomenon.

We have performed a thorough investigation of the variability characteristics of 475 sources, provided by the MASIV survey, to establish whether this phenomenon generally enhances the variability of compact radio sources. On the basis of this study, we conclude that solar-elongation-related variability provides a significant contribution to the total variability, especially for $\epsilon < 30°$. As expected, the effect is most prominent for sources at low ecliptic latitude. We estimated that for sources with $\beta \sim 0°$ the variability increases by a factor of two over the average source modulation index as they pass from the maximum to the minimum solar elongation. The findings of the present study may have important implications for future large-area sky monitoring surveys (e.g. the proposed ASKAP VAST Survey; see Chatterjee et al. 2010).

The nature of the variability is not yet completely understood. We considered whether either weak scattering or strong scattering from refractive scintillation in the vicinity of the Sun are possible causes of the phenomenon. In the first case, a very slow component of the solar wind (with speed of the order of 10 m per second) would be needed to explain the observed variability characteristics. The refractive scintillation model, instead, implies that very small structures exist in the interplanetary plasma. These conditions are unlikely and inconsistent with previous studies in the literature. We also considered whether the change of variability is due to propagation effects in the Earth's bow shock. The deduced values of v and $r_{\rm diff}$ are inconsistent with the expected ones.

We hypothesize that a change in the average parameters of the solar wind along the line-of-sight to the sources may provide a possible explanation of the long timescale of the observed variability.

The strong correlation found in the Urumqi data between the measurement error in single sub-scans and modulation index may be evidence of a link between IPS (whose variability timescale is comparable to the duration of a sub-scan) and the long-term variability. A similar kind of investigation carried out for the MASIV data seems to support this idea. However, alternative interpretations in terms of an *indirect* effect of the Sun, or either atmospheric or even telescope-related effects cannot be excluded. To discriminate between the different hypotheses, further investigations are needed.

Acknowledgements. This paper made use of data obtained with the 25 m Urumqi Observatory (UO) of the National Astronomical Observatories (NAOC) of the Chinese Academy of Sciences (CAS). Liu X. is supported by the National Natural Science Foundation of China under grant Nos. 10773019 and 11073036 and the 973 Program of China (2009CB824800). We would like to thank Peter Müller who provided the software for the processing of the Urumqi raw data. We would also like to thank Dr. Jim Lovell for providing us with the MASIV data and Dr. Hayley Bignall, Dr. Emmanouil Angelakis, Dr. Lars Fuhrmann and Dr. Axel Jessner for the stimulating discussions and suggestions.

References

Bignall, H. E., Jauncey, D. L., Lovell, J. E. J., et al. 2003, ApJ, 585, 653
Chatterjee, S., Murphy, T., & VAST Collaboration 2010, BAAS, 42, 515
Coles, W. A., Liu, W., Harmon, J. K., & Martin, C. L. 1991, J. Geophys. Res., 96, 1745
Dennett-Thorpe, J., & de Bruyn, A. G. 2000, ApJ, 529, L65
Dennett-Thorpe, J., & de Bruyn, A. G. 2002, Nature, 415, 57
Edelson, R. A., & Krolik, J. H. 1988, ApJ, 333, 646
Gabányi, K. É., Marchili, N., Krichbaum, T. P., et al. 2007, A&A, 470, 83
Heeschen, D. S. 1984, AJ, 89, 1111
Heeschen, D. S., Krichbaum, T., Schalinski, C. J., & Witzel, A. 1987, AJ, 94, 1493
Kraus, A. 1997, Ph.D. Thesis, Bonn University, Germany
Kraus, A., Quirrenbach, A., Lobanov, A. P., et al. 1999, A&A, 344, 807
Lazio, T. J. W., Waltman, E. B., Ghigo, F. D., et al. 2001, ApJS, 136, 265
Lazio, T. J. W., Ojha, R., Fey, A. L., et al. 2008, ApJ, 672, 115
Lehar, J., Hewitt, J. N., Burke, B. F., & Roberts, D. H. 1992, ApJ, 384, 453
Lomb, N. R. 1976, Ap&SS, 39, 447
Lovell, J. E. J., Jauncey, D. L., Bignall, H. E., et al. 2003, AJ, 126, 1699
Lovell, J. E. J., Rickett, B. J., Macquart, J.-P., et al. 2008, ApJ, 689, 108
Marchili N. 2009, Ph.D. Thesis, Bonn University, Germany
Marchili, N., Krichbaum, T. P., Liu, X., et al. 2008 [arXiv:0804.2787]
Marchili, N., Martí-Vidal, I., Brunthaler, A., et al. 2010, A&A, 509, A47
Narayan, R. 1992, Roy. Soc. London Philos. Trans. Ser. A, 341, 151
Narayan, R., Anantharamaiah, K. R., & Cornwell, T. J. 1989, MNRAS, 241, 403
Qian, S.-J., & Zhang, X.-Z. 2001, Chinese J. Astron. Astrophys., 1, 133
Quirrenbach, A., Witzel, A., Wagner, S., et al. 1991, ApJ, 372, L71
Quirrenbach, A., Witzel, A., Krichbaum, T. P., et al. 1992, A&A, 258, 279
Raiteri, C. M., Villata, M., Larionov, V. M., et al. 2008, A&A, 480, 339
Readhead, A. C. S. 1971, MNRAS, 155, 185
Rickett, B. J., Witzel, A., Kraus, A., et al. 2001, ApJ, 550, L11
Rickett, B. J., Lazio, T. J. W., & Ghigo, F. D. 2006, ApJS, 165, 439
Scargle, J. D. 1982, ApJ, 263, 835
Senkbeil, C. E., Ellingsen, S. P., Lovell, J. E. J., et al. 2008, ApJ, 672, L95
Simonetti, J. H., Cordes, J. M., & Heeschen, D. S. 1985, ApJ, 296, 46
Sun, X. H., Reich, W., Han, J. L., et al. 2006, A&A, 447, 937
Villata, M., Raiteri, C. M., Kurtanidze, O. M., et al. 2002, A&A, 390, 407
Wagner, S. J., & Witzel, A. 1995, ARA&A, 33, 163
Witzel, A., Heeschen, D. S., Schalinski, C., & Krichbaum, T. P. 1986, Mitteilungen der Astronomischen Gesellschaft Hamburg, 65, 239